

# Tidal tilt observations in the Netherlands using shallow borehole tiltmeters

R. Sleeman<sup>1</sup>, H. W. Haak<sup>1</sup>, M. S. Bos<sup>2</sup>, and J. J. A. van Gend<sup>1</sup>

<sup>1</sup>Royal Netherlands Meteorological Institute (KNMI), P.O. Box 201, 3730 AE, Netherlands

<sup>2</sup>Proudman Oceanographic Laboratory, Birkenhead, Wirral, CH43 7RA, United Kingdom

Manuscript published in  
**Physics and Chemistry of the Earth**  
Vol. 25, No. 4, pp. 415-420, 2000

**Offset requests to:**  
R. Sleeman  
Royal Netherlands Meteorological Institute

# Tidal tilt observations in the Netherlands using shallow borehole tiltmeters

R. Sleeman<sup>1</sup>, H. W. Haak<sup>1</sup>, M. S. Bos<sup>2</sup>, and J. J. A. van Gend<sup>1</sup>

<sup>1</sup>Royal Netherlands Meteorological Institute (KNMI), P.O. Box 201, 3730 AE, Netherlands

<sup>2</sup>Proudman Oceanographic Laboratory, Birkenhead, Wirral, CH43 7RA, United Kingdom

**Abstract.** A small scale experiment with borehole tiltmeters above a gasfield in the Netherlands is described. Pressure variations in the gasfield may cause subsurface deformations leading to tilt. We describe the technique of the installation of the tiltmeters and the influence of the surface conditions on the measurements. For this case study we quantify the minimum pressure variation which is required to result in observable, induced tilt. Tidal tilt observations are shown and used for the verification of the measurements. Finally, we compare the observations with computed ocean tide loading tilt for the M2 tidal component.

## 1 Introduction

Tilt is the inclination or dip of the surface of the Earth. Processes in the Earth which can cause tilt are: the response of the Earth to surface loads, subsurface deformations, tectonic processes and Earth tides. Therefore, tilt measurements are relevant when these types of geophysical processes are being investigated.

A number of experiments with tiltmeters has been carried out recently, with purposes ranging from tidal tilt measurements in a small array (Kohl and Levine, 1995; Wyatt and Berger, 1980) to monitoring induced tilt by groundwater pumping to investigate hydrological processes (Kümpel et al., 1996). Tilt associated with volcanic activity is monitored and described by a number of researchers (e.g. Bonaccorso and Gambino (1997); Westerhaus et al. (1998)). For crustal modeling high accuracy tidal tilt measurements are required. For this purpose a comparison of tiltmeters is described by Wyatt et al. (1982) and Weise et al. (1999). Recalibration of tiltmeters to increase the accuracy of the tilt measurements is described by Mentès et al. (1996).

*Correspondence to:* R.Sleeman (sleeman@knmi.nl)

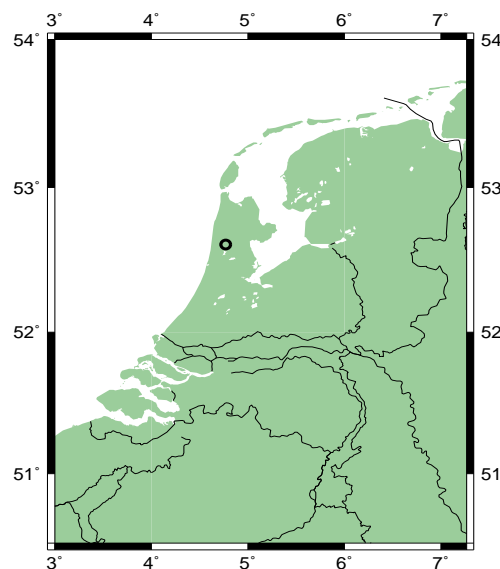


**Fig. 1.** Geographical map of the Netherlands. The circle indicates the geographical area of the tilt experiment.

In 1997 the Seismology Division of the Royal Netherlands Meteorological Institute (KNMI) initiated a small scale experiment with borehole tiltmeters. The purpose of this experiment is to investigate the feasibility of measuring tilt in the Netherlands in a situation where, on a time scale of several days, subsurface deformations are expected. For this purpose we have selected a nearly depleted gas reservoir in which gas is being stored through injection. Pressure variations during this process or during extraction of gas in times of high demand may cause subsurface deformations. Two borehole tiltmeters were installed above the boundary of the gasfield where maximum tilt is expected.

**Table 1.** Tiltmeter sites

	Site A	Site B
Installation depth	5 m	8 m
Surface	asphalt layer (100m x 100m)	grass
Casing	double, PVC plastic	single, steel
Casing diameter	130 mm	220 mm

The gasfield is close to the coast of the Netherlands, at a distance of about 10 km (figure 1). Tidal tilt observations provide an excellent tool for the verification of the measurements, and therefore are important observations in this experiment. Also, the proximity of the coast enables us to investigate the effect of ocean tide loading. At one site a gravimeter was installed to verify the tidal observations.

This paper describes the technique of installing the borehole tiltmeters, presents the influence of the surface conditions and shows tidal tilt observations obtained during this experiment.

## 2 Small scale tilt experiment

The selected gasfield stretches in horizontal directions over about 5 km by 2 km, at a depth of about 2 km and a thickness of about 100 m. A model study of such a gas reservoir by Haak (1996), in which a fully elastic response of the subsurface is assumed, indicates that the largest tilt values are expected above the boundaries of the reservoir. A pressure fluctuation of 1 bar leads in this model to a maximum tilt of about 70 nrad. Therefore we selected two sites (table 1) in the region where maximum tilt is expected, separated from each other by only 1 km. At each site we installed a two-component borehole tiltmeter, for which the technical details are given in table 2. The surface geology (0 - 8m) at both sites is characterized by unconsolidated material like clay, small layers of peat and sand. No other calibrated measurements are available at the tiltmeter sites, except from temperature measurements at a distance of about 20 km.

**Table 2.** Instrumentation

Tiltmeter	Applied Geomechanics Model 722 borehole
Size	85 cm long, 5.4 cm diameter
Weight	6.8 kg
Material	stainless steel
Resolution	3.1 nrad
Range	+/- 80 $\mu$ rad
Power supply	+/- 12V
Output	+/- 8V
Gravimeter	Lacoste Romberg Type D

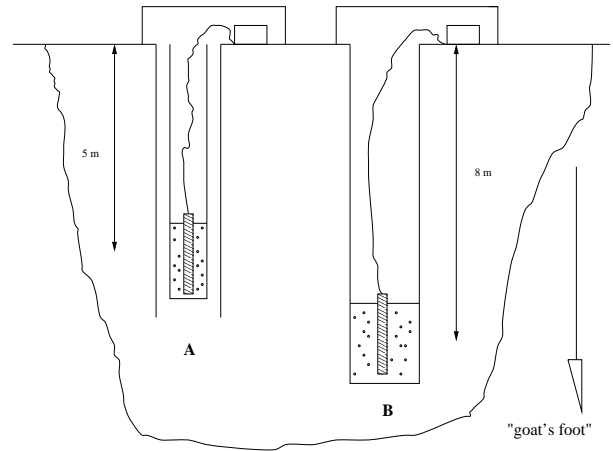


**Fig. 2.** Schematic layout of borehole casings with installed tiltmeters. Tiltmeters are fixed in the double (A) and single (B) cased boreholes with sand. Boreholes and electronics are protected by a sturdy cover.

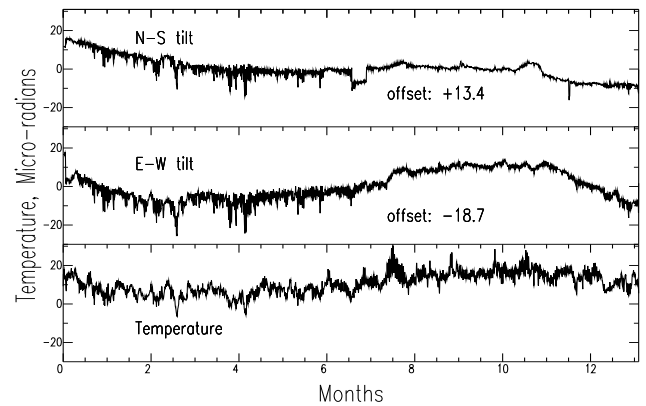


**Fig. 3.** Tilt observations at site A over a period of 13 months and temperature observations at 20 km distance. N-S is the north-south direction, E-W is east-west. A positive tilt means a tilt in the North or East direction.

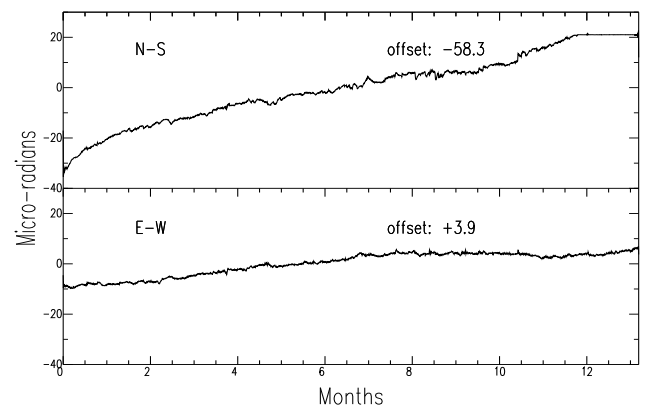


**Fig. 4.** Tilt observations at site B over a period of 13 months. Note that the N-S tilt component is clipped during the last month.

### 3 Tiltmeter installation

Two different types of borehole casings were used to install the tiltmeters, as depicted in figure 2. Tiltmeter A is installed in a double PVC cased borehole. The outer casing is open on both ends, and prevents the borehole from collapsing. The inner casing is sealed on the bottom end and keeps the tiltmeter in a dry environment. We prepared the borehole manually by removing soil material with a soil drill. The drill has a diameter slightly less than the PVC casing as to optimize the mechanical coupling between the casing and its surroundings. After each few decimeters of drilling we forced the PVC casing further downward into the borehole. Each PVC casing had a length of about 2 m, therefore we coupled 3 casings during the process of drilling to reach a depth of more than 5 m. Finally the one-sided sealed inner casing was lowered into the borehole using a heavy weight to overcome the buoyancy of the groundwater. The space between the two casings was filled with coarse sand to optimize the mechanical coupling between both casings.

Site B consists of a single steel cased borehole, which is closed at the bottom end. The casing is driven into the Earth using a mechanical pile-driver. This machine does not remove any soil material but penetrates the casing into the soil using a falling weight.

Next, the tiltmeter is lowered along a cable and positioned in the center just above the bottom of the casing. Dry sand is poured into the casing as to fix the tiltmeter in nearly vertical position. Optimizing its vertical position is done by poking the sand with a tapered probe ("goat's foot") which produces both vertical and lateral forces. The azimuthal orientation of the tiltmeter is determined from the handle on top of it, with an accuracy of a few degrees. At the end of the experiment we were able to extract the tiltmeters from the two boreholes, by simply removing the sand with a vacuum cleaner.

Each tiltmeter contains two orthogonal electrolytic precision tilt sensors to measure tilt in two perpendicular directions. The analog output of each component of the tiltmeter is digitized and sampled at each second, and collected by a PC-based data acquisition system. The tiltmeters can operate in low and high gain mode, and with a selectable lowpass filter at 20 or 0.1 Hz (Applied Geomechanics Inc., 1992). In this experiment we set both tiltmeters in high gain mode, and selected the low frequency lowpass filter. The system has a resolution of 3.1 nrad in the range between -80 to +80  $\mu$ rad.

Site A is equipped with an uncalibrated Lacoste-Romberg model D gravimeter to observe fluctuations in the vertical component of the gravity field. The output is also digitized and sampled at 1 sample per second.

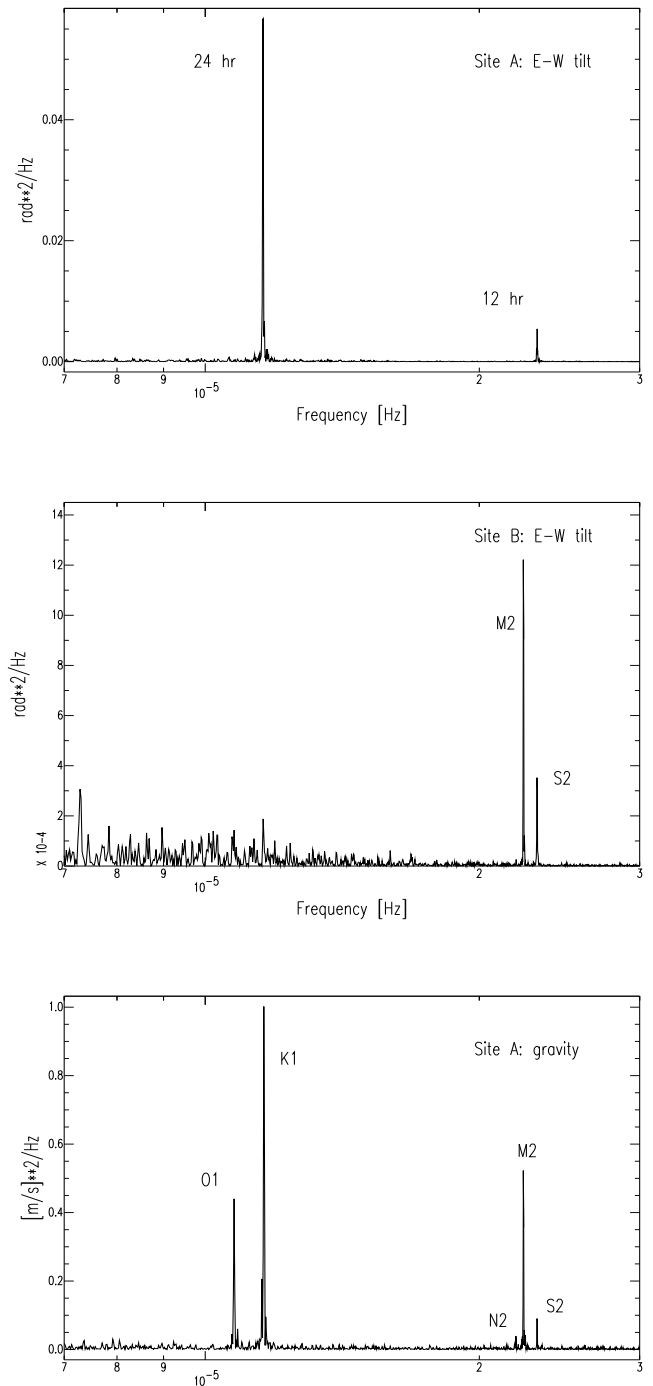


**Fig. 5.** From top to bottom are shown the power spectra of (a) E-W tilt at site A, (b) E-W tilt at site B, and (c) gravity measurements at site A. Notice the difference between the scale factors of the power density axes in (a) and (b).

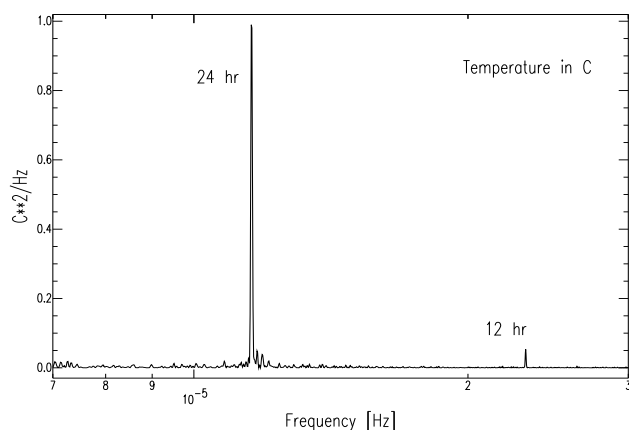


**Fig. 6.** Power spectrum of temperature at a weather station nearby site A.

#### 4 Observations

Tilt time series for sites A and B are shown in figures 3 and 4 between Oct 1997 and Nov 1998. Figure 3 displays the air temperature at a distance of 20 km as well. The measurements at site A clearly contain high frequency components of large amplitude as compared to the tilt signals at site B, and correlate with the high frequency temperature fluctuations as is shown below. This observation is more pronounced during the cold period than during the warm period. Long term tilt at site A closely follows the seasonal temperature changes. This effect is also visible at site B, although less pronounced. Figure 5 shows the power spectra of the E-W tilt components, as well as the power spectrum of the gravimeter measurements, roughly between periods of 9 and 40 hours. The power spectrum of the temperature at the nearby weather station is shown in figure 6 for the same frequency range.

The power spectrum of the gravimeter measurements clearly shows the tidal components O1, K1, N2, M2 and S2, however the tilt spectrum at site A does not show these tidal harmonics. Instead the spectral peaks are here at periods of exactly 12 and 24 hours, and coincide with the peaks in the power spectrum of the temperature. Obviously, the tilt fluctuations at site A reflect temperature induced tilt, caused by the asphalt layer. The asphalt layer contracts and expands due to temperature fluctuations, leading to stress in the subsurface which causes local tilt changes. The peak at 24 hours is caused by the daily fluctuation of the temperature, and the peak at 12 hours represents a higher harmonic. We observe other higher harmonics at 8 hours, 6 hours, 4 hours etc. The influence of the surface conditions on tilt measurements has been observed in other experiments as well (e.g. Kumpel et al., 1996). The power spectrum at site B indicates that this site is less sensitive for

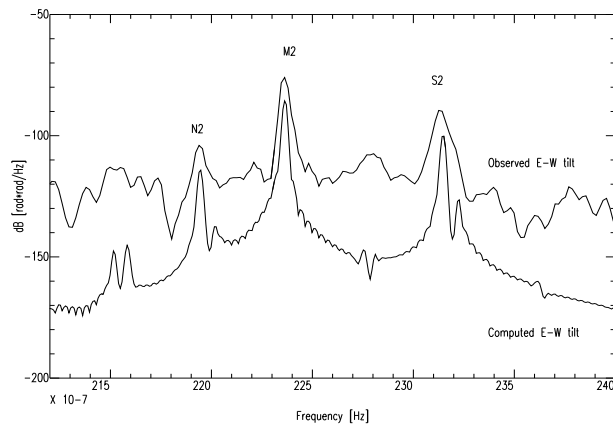


**Fig. 7.** Power spectra of E-W components of observed tilt and theoretical body tide tilt at site B.

temperature fluctuations. Both tilt components clearly measure the M2 and S2 tidal harmonics, but do not show temperature induced tilt in this frequency range.

We used the Earth tide data processing package ETERRA (Wenzel, 1996) to calculate the theoretical tidal tilt at site B for an elastic Earth, using the tidal potential of Tamura (1987). The power spectra of the observed and the theoretical E-W time series are shown in figure 7, for frequencies around the semi-diurnal harmonics. The observed tilt power spectrum shows the harmonics M2, S2 and N2, which clearly contain more energy than the computed ones. This is observed in the N-S tilt component as well.

The additional tilt may be generated by ocean tides. Oceans respond dynamically to the tidal forces (Baker, 1984) and give periodic loads on the Earth's surface. This causes additional tilt with the same frequency as the body tide tilt. We computed tilt variations at site B due to ocean tide loading using four different tide models: CSR3.0, CSR4.0, FES94.1 and FES95.2. For these calculations the PREM elastic Earth model is used and the watermass is conserved. Table 3 shows M2 tilt amplitudes for observed and modeled tilt for the tide models. Notice that for models FES94.1 and FES95.2 the difference between the observed and computed M2 tilt is only 2% for the E-W direction and 6% for the N-S direction. Loading effects of the same order are reported by Agnew (1986) for the east coast of the United States. An M2 loading map for Europe by Baker (1980) reports slightly higher values within the Netherlands.

The above tidal tilt observations illustrate the successful coupling of the tiltmeter at site B to its surrounding. However, the question whether pressure variations in the gasfield may result in observable tilt is still an open question. We estimated the rms of the tilt using a number of series of 6 days of recordings. The rms values for both components are about 0.2  $\mu$ rad and are indicative

**Table 3.** Tilt amplitudes in nrad for observed and computed M2 tides. (O = Observed; B = Calculated body tide; The values at models CSR3.0, CSR4.0, FES94.1 and FES95.2 include body tide tilt and loading tide tilt).

	O	B	CSR3.0	CSR4.0	FES94.1	FES95.2
E-W	96.45	32.15	104.58	106.38	98.65	98.31
N-S	71.51	25.54	76.10	80.71	75.77	75.73

for the noise conditions at site B in this time window. Given these noise conditions, the above model requires a pressure pulse of about 6 bar to produce observable, induced tilt at site B with an amplitude of twice the rms. Such a pressure pulse has not occurred during the experiment.

## 5 Discussion and conclusions

Site conditions are critical for obtaining useful tilt measurements. The asphalt layer at site A clearly introduces temperature induced tilt, which is regarded as noise in this experiment. As this noise contaminates the diurnal and semi-diurnal tidal tilt observations, the coupling of this tiltmeter to its surroundings can not be verified. Hence, only data from site B can be interpreted.

Semi-diurnal tidal tilt components are clearly observed at site B. The amplitude discrepancies between the observed and theoretical M2 tilts in N-S and E-W directions are factors 2.8 and 3.0 respectively. Ocean tide loading may be responsible for this factor, as model calculations for this process are in agreement with the observations. The observations indicate an equal preference for models FES94.1 and FES95.2. The amplitude errors between the observed and the modeled tilts are of the same order of the calibration error as reported by Mentès et al. (1996). The tidal tilt observations at site B show the successful coupling of the single cased steel borehole and the tiltmeter to its surroundings.

The observed rms noise level of about 0.2  $\mu$ rad at site B specifies the feasibility of observing tilt caused by pressure variations in the gasfield. In the model, pressure variations of about 6 bar and more will produce tilt above a detectable level. No such pressure pulses occurred during the experiment. The observed noise may be related to thermoelastic deformation, air pressure fluctuations and pore pressure variations. Removing these types of tilt noise from the observations may lower the detection level for induced tilt.

Possible processes causing the observed tilt, like tectonic deformation or reservoir pressure fluctuations, can not be distinguished using this station only. Therefore, we installed a third tiltmeter recently in the same way as at site B, at a distance of approximately 1.2 km. Data will become available soon and will enable us to investigate the coherence of tilt parameters at both sites.

Long term tilt signal is observed by Weise et al. (1999)

using an Askania borehole tiltmeter at 63 m depth. It is characterized by stable, seasonal drift directions, with large changes in drift taking place in a few days. We do not observe large seasonal drift changes at site B. Our observations show that long term tilt at both sites follow the seasonal fluctuations in temperature. This effect is less pronounced in the deeper borehole. Moreover, the drift at site B has an additional stable component in northeast direction. This direction is in agreement with the tectonic movement of the top of the Pleistocene sands in this area as discussed by Kooi et al. (1998). However, as the observed rate of about 50  $\mu$ rad per year is 2 orders of magnitude larger than inferred from underground benchmarks, the observed rate must be related to subsurface processes.

*Acknowledgements.* This experiment is supported by the Netherlands Ministry of Economic Affairs. The authors thank Amoco Nederland B.V. for their cooperation in this experiment. Comments and suggestions for improvement by the reviewers are gratefully appreciated.

## References

- Agnew, D. C. (1986) Strainmeters and tiltmeters. *Rev. Geophys.*, 24, 579-624.
- Applied Geomechanics Incorporated (1992) *Product Documentation*, 1336 Brommer Street, Santa Cruz, CA 95062, USA.
- Baker, T. F. (1980) Tidal tilt at Llanrwst, North Wales: tidal loading and Earth structure. *Geophys. J. R. astr. Soc.*, 62, 269-290.
- Baker, T. F. (1984) Tidal deformations of the Earth. *Sci. Prog. Oxf.*, 69, 197-233.
- Bonaccorso, A. and Gambino, S. (1997) Impulsive tilt variations on Mount Etna Volcano (1990-1993). *Tectonophysics*, 270, 115-125.
- Haak, H.W.(1996) Tiltmeting een alternatief voor waterpassing? *Technisch rapport TR-192, KNMI*.
- Kohl, M. L. and Levine J. (1995) Measurement and interpretation of tidal tilts in a small array. *J. Geophys. Res.*, 100, 3929-3941.
- Kooi, H., Johnston, P., Lambeck, K., Smither, C. and Molendijk, R. (1998) Geological causes of recent ( $\sim 100$  yr) vertical land movement in the Netherlands. *Tectonophysics*, 299, 297-316.
- Kümpel, H-J., Varga, P., Lehmann, K. and Mentès, G. (1996) Ground tilt induced by pumping - preliminary results from the Nagycenk test site, Hungary. *Acta Geod. Geoph. Hung.*, 31, 67-78.
- Mentès, G., Lehmann, K., Varga, P. and Kümpel, H-J. (1996) Some calibration of the Applied Geomechanics Inc. borehole tiltmeter model 722. *Acta Geod. Geoph. Hung.*, 31, 79-89.
- Tamura, Y. (1987) A harmonic development of the tide generating potential. *Bull. d'Inf. Marées Terr.*, 99, 6813-6855.
- Weise, A., Jentzsch, G., Kiviniemi, A. and Kääriäinen, J. (1999) Comparison of long-period tilt measurements: results from the two clinometric stations Metsähovi and Lohja, Finland. *J. Geodynamics*, 27, 237-257.
- Wenzel, G. (1996) The nanogal software: Earth tide data processing package ETERNA 3.30. *Bull. d'Inf. Marées Terr.*, 124, 9425-9439.
- Westerhaus, M., Rebscher, D., Welle, W., Pfaff, A. and Koerner, A. (1998) Deformation measurements at the flanks of Merapi Volcano. *DGG-Sonderband III/1998, Decade volcanoes under investigation*, 1. Merapi-Galeras Workshop, 93-99.

Wyatt, F. and Berger, J. (1980) Investigations of tilt measurements using shallow borehole tiltmeters. *J. Geophys. Res.*, 85, 4351-4362.

Wyatt, F., Cabaniss, G. and Agnew, D. C. (1982) A comparison of tiltmeters at tidal frequencies. *Geophys. Res. Lett.*, 9, 743-746.